



Sodium Salt-Splitting Performance of a Novel Ceramic-Polymer Composite Cation-Selective Membrane

L. M. Cormier,^{a,c,z} F. Ma,^{a,*} S. T. Bah,^a S. Guétre,^{a,e} M. Meunier,^a
M. Paleologou,^{b,*} and A. Yelon^{a,*}

^aDepartment of Engineering Physics and Groupe des Couches Minces, École Polytechnique de Montréal, Montreal, Quebec, Canada H3C 3A7

^bPulp and Paper Research Institute of Canada (PAPRICAN), Pointe-Claire, Quebec, Canada H9R 3J9

The salt splitting performance of an electrolysis cell incorporating a novel composite membrane consisting of a thin film of an amorphous ceramic with NASICON composition ($\text{Na}_{1+x}\text{Zr}_2\text{Si}_x\text{P}_{3-x}\text{O}_{12}$, $0 \leq x \leq 3$) deposited on commercial cation-selective polymeric membranes was evaluated. We have investigated how the ceramic film thickness and the technique of deposition affected the base current efficiency (BCE) for the production of sodium hydroxide from sodium sulfate. It was found that when full coverage of the polymeric substrate was achieved, the ceramic film improved the salt-splitting performance of the polymeric membrane, even when localized surface defects were present. The study showed that the BCE of the electrolysis cell was the same whether the cation-selective composite membrane used was formed by pulsed laser deposition or by sputtering. Operating the cell above room temperature, and at a high anolyte concentration increased the base current efficiency for sodium hydroxide production.

© 2001 The Electrochemical Society. [DOI: 10.1149/1.1427078] All rights reserved.

Manuscript submitted June 25, 2001; revised manuscript received August 28, 2001. Available electronically December 10, 2001.

A novel cation-selective ceramic-polymer composite membrane was recently proposed for electromembrane systems used in the separation and regeneration of chemicals.¹ For example, processes such as electrolysis and bipolar membrane electro dialysis employing composite cation-selective membranes could be used to recover sodium hydroxide and sulfuric acid from the sodium sulfate by-product generated by chlorine dioxide generators in kraft pulp mills.² To be economically attractive, an electromembrane system must display high energy efficiency and require minimal maintenance during an extended, useful lifetime. The selectivity of a membrane is a key property for achieving these goals because it acts on two levels: (i) the selectivity of the membrane for Na^+ ions over H^+ ions directly affects the current efficiency, and (ii) the selectivity for Na^+ over multivalent ions delays fouling and increases the lifetime of the membrane. Fouling occurs through the formation of insoluble hydroxide salts inside the membrane thereby increasing the electrical resistance of the membrane, and requiring its premature replacement.

At present, electromembrane systems primarily use ion-selective membranes which are entirely polymeric. Two desirable features of polymer membranes are their low electrical resistance and their mechanical flexibility. Their drawbacks are that their selectivity to alkali metal ions declines with increasing acid concentration in the feed compartment^{2,3} and that they degrade at high temperatures. Sodium-selective ceramic membranes provide enhanced current efficiencies and can operate at high temperatures without being damaged.⁴ However, the thickness required for self-supporting ceramic membranes leads to high resistance and increases the energy consumption to unacceptable levels.

The proposed composite membrane consists of a thin film of a ceramic of NASICON composition ($\text{Na}_{1+x}\text{Zr}_2\text{Si}_x\text{P}_{3-x}\text{O}_{12}$, $0 \leq x \leq 3$) deposited on a cation-selective polymeric membrane. We have previously shown⁵ that the presence of this ceramic thin film on a polymer membrane increases current efficiency and prevents fouling. The composite membrane combines the advantages of both polymer (mechanical flexibility and low electrical resistance) and ceramic (Na^+/H^+ selectivity and low multivalent ion fouling rates)⁵ membranes. In the initial phase of the study, the composite mem-

branes were produced by pulsed laser deposition (PLD)⁶ and their performance showed an improvement over that of unmodified polymer membranes.⁵ Composite membranes can also be obtained using the more conventional rf magnetron sputtering technique. Building on the initial results, the objectives of the present study were to (i) determine if there are changes in the performance of the membrane when a different deposition technique is used, (ii) determine the optimal film thickness for the intended applications, (iii) evaluate the membrane at a higher temperature of operation (55°C) and sodium sulfate concentration (1.5 M), and (iv) compare the performance of R-4010® as the polymeric component of the composite membrane to other ion-exchange polymeric membranes of similar composition.

Experimental

Production of composite membranes.—Cation-selective fluorocarbon polymeric membranes (Pall Corporation, NY) were used as substrates for the ceramic deposition (Table I). A small piece of silicon wafer covered by a silicon nitride film was coated alongside the polymeric substrate to serve as a reference for ceramic film thickness measurements. The ceramic thin films were deposited by PLD or by rf magnetron sputtering from bulk NASICON ($\text{Na}_3\text{Zr}_2\text{Si}_2\text{PO}_{12}$) targets. To prevent severe degradation of the polymeric membrane, the ceramic films were deposited at room temperature with no subsequent annealing. The resulting thin films were amorphous with NASICON-like composition.⁶ The NASICON target fabrication method and the experimental setup for PLD were described elsewhere.^{6,7} The beam of an excimer laser (KrF, 248 nm) was focused on the rotating NASICON target to an elliptic spot size of 2.2 mm². The energy density was adjusted to 0.6 J/cm² at a laser repetition rate of 30 Hz. RF magnetron sputtering was performed at 75 W under 0.67 Pa (5 mTorr) argon pressure. For the thickness study, two series of ceramic films ranging from 40 to 450 nm in thickness were deposited on R-4010 membranes using the two deposition techniques. For other experiments, the ceramic film thickness was in the range determined to be optimal from the results of the thickness study, 70–100 nm.

X-ray photoelectron spectroscopy (XPS) was performed on a VG Escalab MKII, calibrated with the Ag 3d_{3/2} line at -368.3 eV. Non-monochromatized Mg K α (1256.3 eV) radiation from a dual anode was used as the X-ray source. The source was generally operated at 15 kV, 20 mA, and was sometimes used at 12 kV, 10 mA to prevent radiation damage to the polymeric membrane. Relative atomic compositions were calculated from low resolution survey scans using the

* Electrochemical Society Active Member.

^c Present address: Pulp and Paper Research Institute of Canada, Pointe-Claire, Quebec, Canada H9R 3J9.

^d Present address: Reveal Inc., Hawthorne, New York 10532, USA.

^e Present address: Iridian Spectral Technologies, Ottawa, Ontario, Canada K1A 0R6.

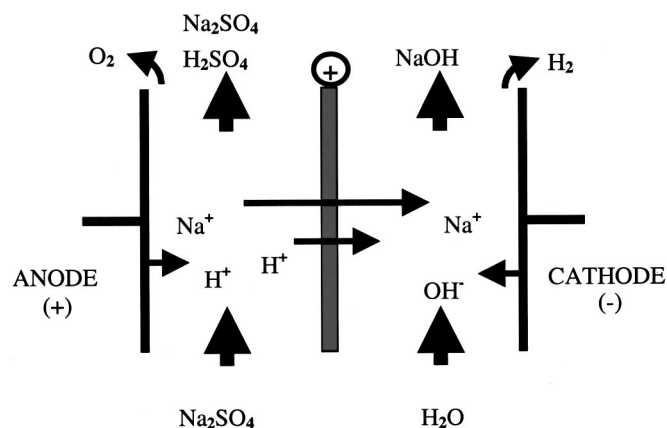
^z E-mail: lcormier@paprican.ca

Table I. Properties of the cation-selective polymeric membranes used in this study.

Polymer	Glass fiber reinforcement	Thickness (mm)	Resistance in 0.6 N KCl (Ω/cm^2)	Ion exchange capacity (meq/g dry)
R-4010	No	0.10-0.13	0.2-1.0	1.5
Ionclad 4010	No	0.07	0.6	1.2
RF-4010	Yes	0.02	1.9	0.1
BCM 4010	No	0.17	2.2	0.9

empirical sensitivity factors published by Briggs et Seah.⁸ Scanning electron microscopy (SEM) images were taken of the composite membranes before and after electrochemical evaluation. Image analysis of SEM micrographs was performed using ImageTool version 2.00 shareware from the University of Texas. The microroughness of the R-4010 membrane was measured using a Talyscan stylus profilometer (Taylor-Hobson, U.K.) on two 1 mm² areas at a 2 μm lateral resolution. The rms roughness was calculated after filtering the surface topography with a Gaussian filter at an 80 μm cutoff wavelength.

Thickness study.—The performance of the composite membrane in the electrolytic splitting of sodium sulfate into sodium hydroxide and sulfuric acid was assessed using a hexagonal stack cell (HSC) (Graver-Aqualytics, NJ). This cell allows operation under industrially representative hydrodynamic conditions. A simplified schematic of an electrolysis cell is presented in Fig. 1 to illustrate the process. In the actual HSC, the distance between the electrodes is small (4 mm). The membrane is sandwiched between two mesh-like spacers designed to maximize contact of the solutions with the membranes. The width of the two compartments was 1 mm and the membrane area was 27 cm². The platinum electrodes were 5.3 cm² area disks. A peristaltic pump provided circulation of the solutions inside the cell at a flow rate of about 100 mL/min, which corresponded to a linear velocity inside the cell of around 4 cm/s. The current density was maintained at 150 mA/cm². The anolyte was a solution 1 M in Na₂SO₄ and 0.7 N in H₂SO₄ and the catholyte was a 1 M NaOH solution. The HSC was run in a simulated feed-and-bleed mode at room temperature (22°C), that is, the volume of the electrolyte compartments was sufficiently large to avoid significant changes in concentrations over time. The acid and base concentrations were determined using titration. Current efficiency is defined as the fraction of the current consumed for the generation of useful chemicals, NaOH in this case. The base current efficiency (BCE) is the ratio of the number of equivalents of Na⁺ ions transferred across the membrane and converted to NaOH, divided by the theoretical (Faraday's law)

**Figure 1.** Simplified schematic illustrating the principle of salt splitting using electrolysis.

number of equivalents of Na⁺ transferred and converted to NaOH for a known charge passed between the two electrodes.

Durability study.—The long-term performance of the composite membrane was evaluated using a two-compartment Plexiglas cell with a working membrane area of 1 cm². The electrolytes and the applied current density were the same as described above. In this cell, the exposed area of the membrane was not compressed between spacers and the linear velocity of solutions in the cell was only 0.02 cm/s. The membrane was positioned with the ceramic film facing the catholyte. Sampling and concentration adjustments were performed weekly for a period of 284 days.

Operation under increased temperature and anolyte concentration.—In order to simulate industrially realistic conditions, some electrolysis experiments were performed using the HSC with an anolyte concentration of 1.5 M Na₂SO₄, maintained at 55°C. The feed compartment was run in the batch mode while the base compartment was in a simulated feed and bleed mode.

Evaluation of alternative membrane substrates.—As the membrane supplier discontinued production of R-4010 during our study, other cation-selective membranes from the same supplier were evaluated as substitutes for R-4010. The membranes had the same ion-exchange groups but differed in thickness and roughness. Table I outlines the principal characteristics of these membranes. A polytetrafluoroethylene (PTFE) membrane (no ion exchange groups) from Electrosynthesis Inc., was also evaluated to ascertain that the ceramic thin film does confer selectivity to such a membrane. The thickness of the ceramic layer on the PTFE membrane was 80 nm. For this set of experiments, the HSC was run at 55°C with an initial anolyte concentration of 1.5 M Na₂SO₄ and the concentration of H⁺ ions was allowed to increase freely during operation (batch mode). The starting concentration of the catholyte was 1 M NaOH. The rest of the operating parameters remained the same as for the thickness study.

Results and Discussion

Characterization of as-deposited ceramic films.—The as-deposited ceramic films and the R-4010 polymeric substrate material were examined by SEM and XPS. SEM micrographs showed that the polymeric substrate had pores which averaged 0.01 μm^2 in area and were randomly distributed (Fig. 2a). The polymer also displayed some smooth texturing on a larger scale. The as-deposited films showed good overall coverage of the substrate, masking the pores completely, but followed the texture of the polymer deposition by PLD (Fig. 2b) and deposition by sputtering (Fig. 2c). The measured rms microroughness of the polymer was ~ 83 nm, setting a threshold thickness at which thin films could fill the local topography. The impact of this is discussed in the Electrochemical evaluation section. Very few film surface defects were present, and these were in the form of pinholes. The samples deposited by PLD appeared rougher

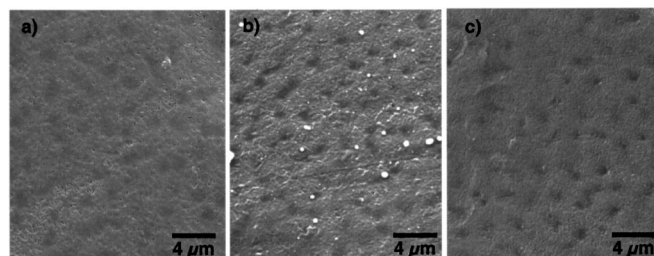
**Figure 2.** SEM micrographs: (a) uncoated R-4010, (b) PLD-deposited ceramic film on R-4010, (c) ceramic on R-4010 deposited by rf magnetron sputtering.

Table II. Comparison of the relative atomic compositions of sodium-selective ceramic thin films deposited on R-4010 membranes and the surface composition of the NASICON target measured by XPS.

Element	Target (atom %)	PLD (atom %)	RF magnetron sputtering (atom %)
Na	10	<1	<1
O	65	65	67
Zr	10	15	11
P	5	5	11
Si	10	15	11

than the sputtered samples and had particles on their surface. These particles are inherent to the PLD process and increase in size and number with increasing thickness.^{6,7,9}

The ceramic films deposited were amorphous, as was expected from their deposition energy density $<1 \text{ J/cm}^2$ and the low substrate temperature.⁶ Evaluation of the chemical composition of the films by XPS showed good transfer of stoichiometry from the target to the sample by either PLD or sputtering. Table II presents the relative atomic compositions of typical ceramic films deposited on polymeric membranes by both techniques as well as the measured surface composition of the target. The ceramic thin films deposited on the cation-selective membranes were depleted in sodium at the surface and enriched in Na at the film/substrate interface. The origin of this effect is discussed in an earlier publication.⁶ Aside from this, the ceramic composition did not vary significantly with the thickness of the deposited films.

It is well known that amorphous NASICON materials are not as good ionic conductors as their crystalline counterparts,^{10,11} but for this application the ceramic could not be made crystalline with an annealing cycle because the polymer membrane would severely degrade above 70°C . Since the ceramic films used were very thin, the total resistance of the membrane and hence the energy requirements of the cell remained largely unchanged. The key property is the selectivity of the membrane for Na^+ over H^+ , which is one of the main determinants of current efficiency. Selectivity measurements performed in a chloride environment^{12,13} have shown that the selectivity of crystalline NASICON for Na^+ over H^+ is not as good as compared to its selectivity over K^+ , Li^+ , or Ca^{2+} , but that the Na^+/H^+ selectivity is better than other cation-selective materials. If the selectivity of the composite membrane is higher than that of the polymer alone, there will be an improvement in current efficiency. In a previous publication,⁵ we have demonstrated that the sodium ion conductivity and the Na^+/H^+ selectivity of NASICON-like amorphous thin films are sufficient to improve current efficiency. The conduction mechanism of sodium ions in this material remains to be fully explained and is beyond the objectives of the present study.

Electrochemical evaluation.—The effect of the ceramic thickness and deposition technique on the base current efficiency is shown in Fig. 3. Membranes deposited by sputtering and PLD did not show a significant difference in BCE for a given thickness. Both curves showed a maximum BCE around 70–100 nm and then the BCE steadily declined until it reached a plateau at about 44%. This result indicates that the slight enrichment in phosphorous of the sputtered ceramic as compared to the PLD film did not produce a significant difference in the selectivity of the ceramic. Thus, the ceramic films produced by both techniques can be considered equivalent in terms of sodium selectivity. The optimal range of ceramic film thickness is of the same order as the microroughness of the polymer membrane. Outside the optimal range, the BCE drops either due to lack of coverage of the substrate or because of mechanical failure of the ceramic, as is detailed below. When there was insufficient coverage of the substrate by the ceramic, as for the films thinner than 70 nm, the BCE was characteristic of the uncoated

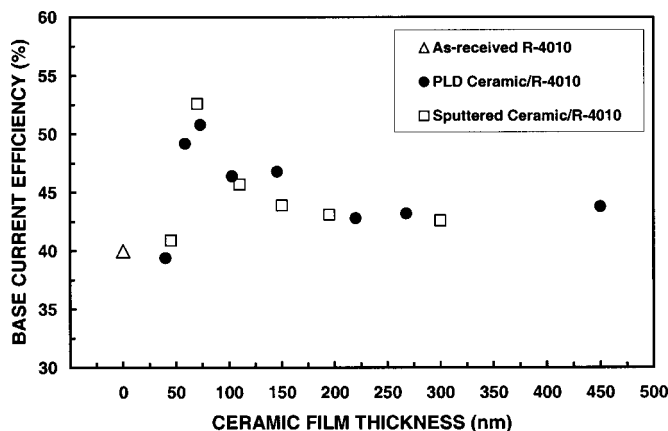


Figure 3. Effect of ceramic thickness and deposition technique on base current efficiency.

membrane and not of the ceramic. Figure 4a gives an example of insufficient coverage of the polymeric membrane by the ceramic film where some pores from the substrate were left exposed after deposition allowing ions to go through the membrane without interacting with the ceramic during electrolysis. Deficient coverage of the substrate was also confirmed by the detection of fluorinated carbon groups by XPS.

For films thicker than the optimal range, the drop in BCE could be attributed to a decrease of ceramic selectivity beyond a threshold thickness, to localized surface defects, or to localized failure of the ceramic causing exposition of the underlying polymer. The last hypothesis was confirmed after microscopic observation of the composite membranes after electrolysis. Portions of the membrane where the ceramic coating was absent represented areas where H^+ ions could cross to the catholyte compartment at higher fluxes because the polymer was not as Na^+/H^+ selective as the ceramic. This decreased the total Na^+ ions transferred and thus the BCE, but did not completely eliminate the beneficial effect of the sodium-selective ceramic film. Figures 4 and 5 display selected SEM micrographs obtained after electrolysis of PLD-deposited and sputtered ceramic films, respectively. SEM observation after electrolysis experiments revealed that cracks had formed in the coating and that new pinholes with smooth edges had been created, as illustrated in Fig. 4. Quantification of the micrographs using image analysis was attempted, but was difficult due to the minimal contrast between the coating and the substrate of some samples. It was estimated that the average pinhole size was sufficiently large to allow transfer. The high BCE values were observed for the films which had defects occupying less than 1% of the surface area examined, and the maximum BCE was obtained for the sample for which no defects could be seen by scanning electron microscopy (Fig. 5a). If the surface defects occupied more than 1% of the total area, then a drop in BCE from the maximum was observed, although the BCE

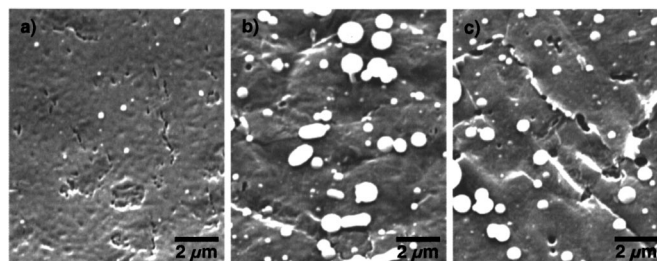


Figure 4. SEM micrographs of PLD-deposited composite membranes after electrolysis. Ceramic film thickness: (a) 60, (b) 240, and (c) 450 nm.

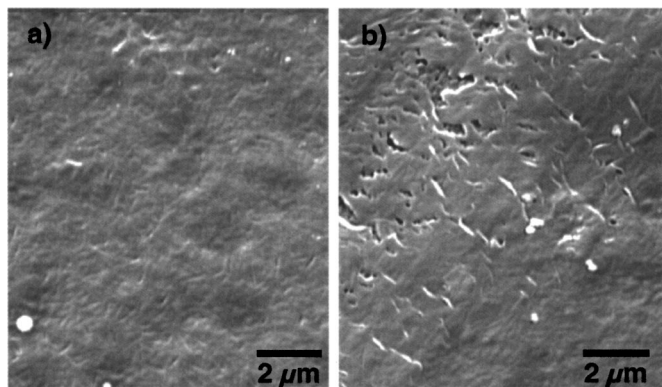


Figure 5. SEM micrographs of sputter-deposited composite membranes after electrolysis. Ceramic film thickness: (a) 70 and (b) 250 nm.

was still 4% higher than for the polymeric membrane alone. The drop in BCE for the composite membrane indicates that its enhanced Na^+/H^+ selectivity, provided by the ceramic film, decreased toward that of the polymeric substrate.

The defects appear to be caused by mechanical as well as by chemical action. PLD films thicker than 100 nm showed a more disrupted surface than the thinner ones, with ruptured film edges overlapping in certain areas, as can be seen in Fig. 4b and c. Swelling of the polymeric membrane upon contact with the electrolyte solution combined with the mechanical stresses linked to the installation of the membrane in the cell, and operation under high fluid flow are factors that could cause the separation of the coating from the polymer. To minimize leakage in the cell, the flexible membrane is highly compressed against the spacer mesh, which acts as many local stress concentrators. As the ceramic film gets thicker, it appears not to be able to withstand these stresses. The imprint of the mesh on the membrane was often observed after removal from the cell. For sputtered samples, mechanical removal of significant portions of the film had occurred such as shown in Fig. 5b, indicating decreased adherence as compared to the PLD samples. From this point of view, sputtered films may not be as suitable for the application as the PLD films.

The smooth-edged pinholes are attributed to some localized chemical dissolution of the ceramic film. XPS analysis of the ceramic films after salt-splitting experiments indicated that the composition of the sputtered films underwent more change than that of the PLD films (Table III). There was a major increase in the surface oxide concentration of the sputtered films and the relative concentrations of P and Zr decreased relative to Si. The mechanical removal of areas of the film discussed in the preceding paragraph also contributed to the decrease in the detected concentrations of the various elements in the ceramic. For the PLD films, the concentration changes were small and consistent with the hypothesis of localized dissolution.

The observed localized dissolution of the film does not spread rapidly, as very good BCE results ($\sim 54\%$) were obtained for over 200 days of operation with a 25 nm PLD-deposited ceramic film

Table III. Typical relative atomic compositions of sodium-selective ceramic thin films deposited on R-4010 membranes after electrolysis.

Element	PLD (atom %)	RF magnetron sputtering (atom %)
Na	3	3
O	67	89
Zr	13	<1
P	4	2
Si	13	6

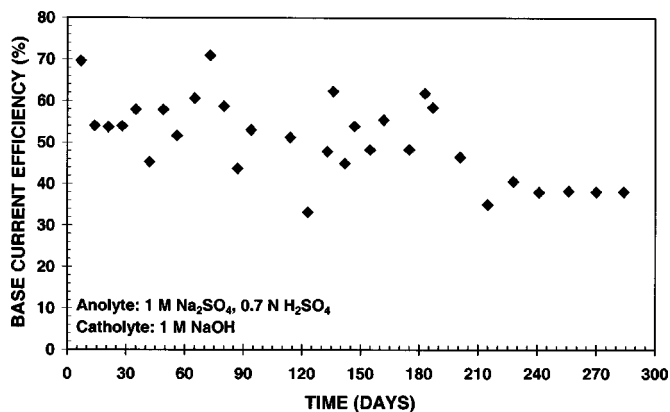


Figure 6. Durability study for the composite membrane with the ceramic facing the catholyte.

facing the catholyte (Fig. 6). SEM and XPS analysis of the sample after the end of the durability test showed that some of the ceramic film remained on the surface, although it was thinned and cracked in many areas (Fig. 7). In this cell, the membrane was under very low mechanical stresses as compared to the HSC, so the degradation in performance is mostly related to chemical action. The drop in BCE starting around 210 days of exposure cannot be entirely attributed to membrane failure because an independent problem occurred with the cell that prompted its disassembly and has probably disturbed the experimental conditions when the cell was put back in operation for the remainder of the test.

Performance of membrane under high operating temperature and Na_2SO_4 concentration.—Figure 8 shows how the base current efficiency for a system incorporating a ceramic PLD-coated or uncoated R-4010 membrane varies with increasing H^+ concentration in the anolyte. At low H^+ concentrations, the cation-selective membranes are in the alkaline state,³ and as a result, the BCE is independent of the H^+ concentration. This explains why the improved Na^+/H^+ selectivity conferred by the ceramic film only begins to be reflected in the BCE when the membranes reach the acidic state. In the acidic state, the BCE declines due to an increased flux of H^+ ions competing with the Na^+ ions in crossing the membrane to the

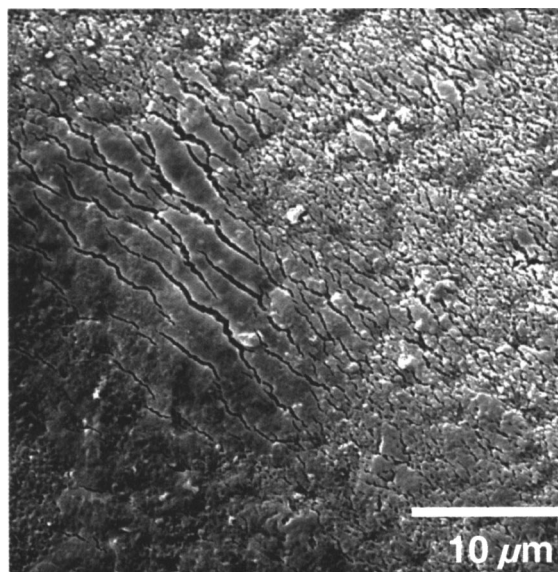


Figure 7. SEM micrograph of the ceramic side of the membrane after 284 days of electrolysis.

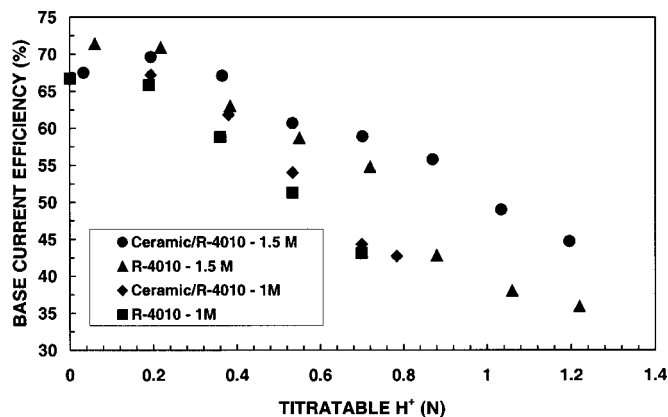


Figure 8. Na₂SO₄ salt-splitting base current efficiency for uncoated and ceramic-coated R-4010 membranes at room temperature. Initial anolyte concentration: 1 or 1.5 M Na₂SO₄; initial catholyte concentration: 1 M NaOH. The feed compartment was run in the batch mode while the base compartment was in a simulated feed and bleed mode.

catholyte compartment. The improved performance of the membranes for 1.5 M Na₂SO₄ anolyte concentration can be explained by the increased buffering capacity of the solution, which reduces the transport of H⁺ ions through the membrane. This is further indicated by the membrane shifting to the acidic state at a higher titratable H⁺ concentration. The presence of the ceramic thin film increased the BCE of the uncoated membrane proportionally more at 1.5 M than at 1 M, with the anolyte compartment run in the batch mode. This is an advantage for industrial applications.

The BCE increased upon heating the anolyte solution to 55°C. Comparing the BCE values at 0.7 N acid, the BCE was about 20% higher at 55°C than at 22°C for both the composite membrane and the uncoated polymer (Table IV). The 20% increase in BCE is comparable to the increase in the ratio of equivalent ionic conductivity of Na⁺/free H⁺. For example, at 25°C this ratio is 6.88 and becomes 5.67 at 50°C.¹⁴ The composite membrane still showed an improvement of about 11% (at 0.7 N acid) over the uncoated polymer, which is comparable to the improvement at room temperature for the same anolyte concentration. The increase in temperature brings an increase in the ratio of equivalent ionic conductivity of Na⁺/free H⁺ in solution, but does not significantly affect the ratio of Na⁺/H⁺ selectivity of the ceramic and the polymer membrane.

Other polymeric membrane substrates.—In order to compare the performance of the different membranes, values of the BCE at 0.7 N H⁺ concentration interpolated from the regression line of the acidic state region were examined. The importance of full surface coverage by the sodium-selective ceramic film is shown again by these results. The performance of the uncoated membranes ranked from best to worst, BCM>RF>R-4010>Ionclad and the coated membranes ranked as R-4010>RF>Ionclad>BCM. The largest improvement of BCE provided by the ceramic thin film is on R-4010 followed by Ionclad. These two membranes are the most similar of the set in terms of electrical properties and surface roughness (Fig. 9). The performance of the RF-4010 was only improved by about 4%, typical of an incompletely covered substrate. The macroroughness cre-

Table IV. Base current efficiency (BCE) at 0.7 N titratable H⁺ concentration for uncoated R-4010 and ceramic/R-4010 composite membranes for 1.5 M Na₂SO₄ anolyte concentration.

Temperature (°C)	R-4010	Ceramic/R-4010
22	52.5	58.0
55	62.9	70.0

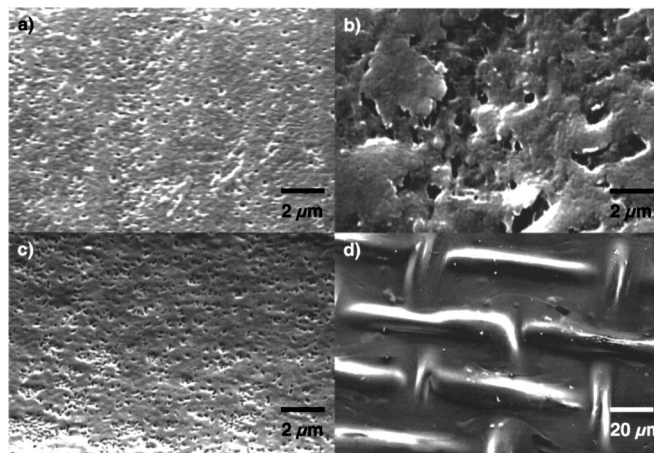


Figure 9. SEM micrographs of other polymeric membranes: (a) Ionclad 4010, (b) BCM 4010 (c) RF-4010, (d) RF-4010 (low magnification).

ated by the glass fiber reinforcement mesh probably explains the difficulty of obtaining complete surface coverage. The poor performance of the coated BCM 4010 membrane is related to deposition-induced degradation of its properties. The surface of the BCM 4010 membrane was very rough and porous, requiring a thick ceramic film to provide full surface coverage. The extended deposition times required to deposit such thick films caused melting of the polymer and degraded the performance of the membrane.

The results of the salt-splitting experiments using a PTFE membrane substrate are shown in Fig. 10. The relatively large porosity of the membrane (30–60 μm), allowing osmotic transport across the membrane, as well as the absence of ion-exchange groups in the membrane made it very difficult to perform the test and explained the very low BCE obtained. It is clear that the deposition of a ceramic layer increased the BCE significantly, it conferred Na⁺/H⁺ selectivity to the PTFE membrane, even though the absolute value is too low to be of practical interest.

Conclusions

The Na⁺/H⁺ selectivity of a polymeric cation-exchange membrane can be enhanced by the deposition of a NASICON-like ceramic thin film on its surface. Optimal current efficiencies for the production of sodium hydroxide from sodium sulfate in an electrolysis cell were obtained when the ceramic layer thickness on R-4010 polymeric membranes was in the 70–100 nm range, and film defects (*i.e.*, cracks, pinholes) occupied less than 1% of the surface. In terms of current efficiency, the ceramic thin films deposited by pulsed laser deposition and rf magnetron sputtering performed similarly under

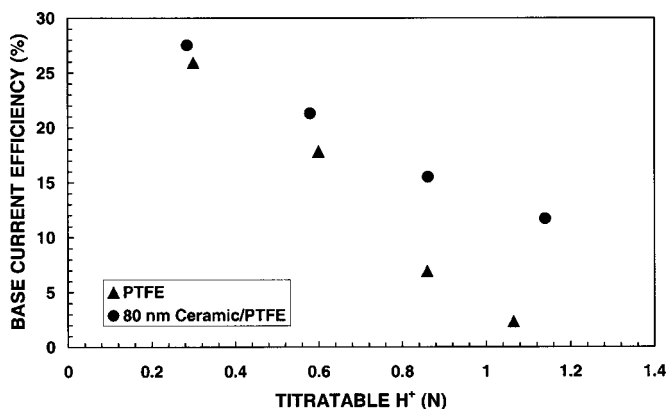


Figure 10. Salt-splitting performance of PTFE and ceramic-coated PTFE.

the electrolysis conditions investigated, although the PLD-deposited films appeared to degrade less (physically and chemically) during electrolysis than the sputtered films. An increase in temperature or anolyte concentration improved the performance of the electrolysis cell, but only the increase in Na₂SO₄ concentration increased the difference in Na⁺/H⁺ selectivity between the composite and the polymer membrane. Of the four polymeric membranes evaluated, R-4010 was the most suitable substrate for this application.

Acknowledgments

The authors gratefully acknowledge the financial support of the Natural Sciences and Engineering Research Council of Canada and the Pulp and Paper Research Institute of Canada. Dr. F. Girard and Dr. R. Izquierdo are thanked for fruitful discussions. E. Quenneville and P.-Y. Wong are thanked for their help with the experimental aspects of PLD and electrochemical testing, respectively.

The Pulp and Paper Research Institute of Canada assisted in meeting the publication costs of this article.

References

1. A. Yelon, M. Paleologou, D. Ivanov, R. Izquierdo, and M. Meunier, *U.S. Pat.* 5,968,326 (1999).
2. M. Paleologou, A. Thibault, P.-Y. Wong, R. Thompson, and R. M. Berry, *Sep. Purif. Technol.*, **11**, 159 (1997).
3. J. Jorissen and K. H. Simmrock, *J. Appl. Electrochem.*, **21**, 869 (1991).
4. D. Sutija, S. Balagopal, T. Landro, and J. Gordon, *Electrochem. Soc. Interface*, **5**(4), 26 (1996).
5. F. Girard, R. Izquierdo, E. Quenneville, S. T. Bah, M. Paleologou, M. Meunier, D. Ivanov, and A. Yelon, *J. Electrochem. Soc.*, **146**, 2919 (1999).
6. R. Izquierdo, E. Quenneville, D. Trigylidas, F. Girard, M. Meunier, D. Ivanov, M. Paleologou, and A. Yelon, *J. Electrochem. Soc.*, **144**, L323 (1997).
7. R. Izquierdo, F. Hanus, Th. Lang, D. Ivanov, M. Meunier, L. Laude, J. F. Currie, and A. Yelon, *Appl. Surf. Sci.*, **96-98**, 855 (1996).
8. D. Briggs and M. P. Seah, *Practical Surface Analysis by Auger and X-Ray Photoelectron Spectroscopy*, p. 511, John Wiley & Sons, New York (1983).
9. R. Izquierdo, Ph.D. Thesis, École Polytechnique de Montréal (1998).
10. J. P. Boilot, P. Colombar, and G. Collin, *Solid State Ionics*, **18-19**, 974 (1986).
11. P. Colombar, *Solid State Ionics*, **21**, 97 (1986).
12. A. Caneiro, P. Fabry, H. Khireddine, and E. Siebert, *Anal. Chem.*, **63**, 2550 (1991).
13. O. Damasceno, E. Siebert, H. Khireddine, and P. Fabry, *Sens. Actuators B*, **8**, 248 (1992).
14. *CRC Handbook of Chemistry and Physics*, R. C. Weast and M. J. Astle, Editors, pp. D-145-D-146, CRC Press, Boca Raton, FL (1981).